Journal of Ceramic Processing Research. Vol. 22, No. 5, pp. 521~526 (2021)
(Received 20 January 2021, Received in revised form 30 April 2021, Accepted 14 May 2021)
https://doi.org/10.36410/jcpr.2021.22.5.521

J O U R N A L O F
Ceramic Processing Research

Synthesis and photocatalytic properties of ZnO@ZIF-8 nanostructured composites

Fengge Song, Yangang Sun* and Pinhua Rao*
College of Chemistry and Chemical Engineering, Shanghai University of Engineering Science, Shanghai 201620, China

A simple solution reaction and calcination methodis explored to synthesize the ZnO@ZIF-8 nanostructured composites and the ZnO@ZIF-8-N_2 nanostructured composites using the ZnO nano/microrods as precursor. The photocatalytic activities of different products were investigated using an aqueous solution of methylene blue (MB) as the pollution at ambient temperature. The results of the photocatalytic activities revealed that the ZnO@ZIF-8 nanostructured composites exhibit the better photocatalytic properties than ZnO nano/microrods and the ZnO@ZIF-8-N2 nanostructured composites. The degradation rates of MB solution over ZnO@ZIF-8 nanostructured composites reached to 97.6% under visible light irradiation.

Keywords: ZnO@ZIF-8, nanostructured composites, photocatalyst.

Introduction

With the further development of industry and agriculture, the environment harm of wastewater containing a large number of organic pollutants is increasingly serious. Therefore, it is necessary to effectively control and reduce the environment damage of organic pollutants. In order to promote the application of photocatalytic technology, various types of photocatalysts have been developed to reduce the emissions of organic pollutants from chemicals, dyes and harmful gases [1-5]. At present, using semiconductors as the photocatalyst to photocatalytic degrade organic pollution in wastewater is an effective method, which is a hot point in the field of environmental remediation [6, 7].

Among all kinds of semiconductor photocatalysts, ZnO with a band gap of 3.2 eV is a typical semiconductor photocatalyst. ZnO is widely used in wastewater treatment due to its thermal stability, non-toxicity and low price [8, 9], but it is still a challenge to inhibit the electron-hole recombination probability of ZnO and reduce its wide band gap [10]. Therefore, different methods, such as morphology adjustment, band gap engineering, nonmetal and metal doping, semiconductor coupling and heterojunction fabrication, have been used to optimize the photocatalytic performance of ZnO [11, 12]. Recently, 2-Methylimidazole zinc salt (ZIF-8) has also been used to construct ZnO-based composite materials. For example, Kim et al. [13] reported that the surface of ZnO nanorod was transformed into crystalline ZIF-8, and the products of ZnO@ZIF-8 NRs were used the experimental process to prepare a UV photodetector. Tian et al. [14] obtained the hollow structure of ZnO@ZIF-8 with superior selectivity and gas response toward acetone due to thin layers of ZIF-8 coating on the surface of ZnO hollow-structure fibers. Yang et al. [15] obtained the hybrid catalysts of ZnO@ZIF-8. The preparation process was the part of ZIF-8 was converted to ZnO by using $AgNO_3$ as the treatment agent, and then to form ZnO@ZIF-8 hybrid catalysts. The ZnO@ZIF-8 photocatalysts exhibit enhanced photocatalytic activities. Wang et al. [16] prepared ZnO@ZIF-8 heterostructure microspheres with size selective photocatalysis properties, and displayed improved selective reduction of Cr(VI) from aqueous solution of dye.

In the work, we used a simple solution reaction and calcination using the ZnO nano/microrods as precursor to get ZnO@ZIF-8 nanostructured composites and ZnO@ZIF-8-N_2 nanostructured composites, respectively. The structure of phase and morphology of the as-obtained products were identified by X-ray powder diffractometer (XRD) and scanning electron microscope (SEM). The photocatalytic activities were also investigated by using aqueous solution of methylene blue (MB) as a probe. As a result, with the evolution of the phase structure and composition from ZnO to ZnO@ZIF-8, the improved photocatalytic properties of ZnO@ZIF-8 nanostructured composites were observed obviously.

Materials and Methods

Synthetic of ZnO nano/microrods

The chemical reagents of the experiment process

*Corresponding author:
Tel : +86-21-67791211
Fax: +86-21-67791211
E-mail: syg021@sues.edu.cn (Y. Sun),
raopinhua@hotmail.com (P. Rao)

were analytical grade without purification. Under the condition of ice water bath, 2.5 mL of 0.2 M sodium dodecylsulfate (SDS) solution were added into 10 mL of 1 M $Zn(NO_3)_2 \cdot 6H_2O$ solution, and then 12 mL of 4 M NaOH solution was added drop by drop under the strong magnetic stirring, finally 50 mL suspension was obtained. The suspension was stirred vigorously at room temperature for 1.5 h. Transfer the suspension to a conical flask, put it into an oven, and react for 5 hours at 85 ºC. After cooling to ambient temperature, the as-prepared white products was centrifuged and washed with distilled water and anhydrous ethanol, respectively. The white ZnO powder was obtained.

Syntheses of ZnO@ZIF-8 nanostructure composites

Under magnetic stirring, 0.0407 g (0.5 mmol) of the above-mentioned catalyst powder was added into 32 mL of the mixture (N,N-dimethylformamide and deionized water in a volume ratio of 3:1), after 30 min, added 0.3284 g (4 mmol) of 2-methylimidazole, and stirred for 0.5 h at ambient temperature, and then reacted at 70 ºC in the oven for 48 h. The white precipitate was centrifuged at room temperature, washed with N,N-dimethylformamide and anhydrous ethanol for three times respectively, and the white ZnO@ZIF-8 powder was prepared. The ZnO@ZIF-8 powder was putted in a tubular furnace, and calcined at 400 ºC for 2 h in N_2 atmosphere. The sample was labeled as ZnO@ZIF-8-N_2.

Characterization

The phase structures of the synthesized samples were determined using a Rigaku D/max2550 PC X-ray powder diffractometer with Cu-Kα radiation at 200 mA and 40 kV. S-4800 scanning electron microscope (SEM) was used to observe the morphologies of the samples. The UV-visible spectra of different samples were detected by UV-3600 UV-visible diffuse reflectance analyzer. The absorbance change of methylene blue solution was measured with UV-1902PC UV-visible spectrophotometer.

Photocatalytic performance test

Methylene blue (MB) aqueous solution was used to the pollutant, and 300 W xenon lamp was used as the light source to simulate the sunlight in this experiment, in order to observe the photocatalytic activities of the sample. The experimental procedure was as follows: The catalyst sample (20 mg) was suspended in MB (5 mg/L, 50 mL; 5 ppm) solution, and the mixture solution was placed in the dark for 35 min to achieve the adsorption-desorption equilibrium. Then the mixture solution was exposed to xenon lamp irradiation, and then 3 mL of the mixture solution was taken and centrifuged every 20 min. The UV-Vis spectrum of MB solution was recorded by a spectrophotometer (UV-1901). After the test, the precipitate and solution were poured back into the reactor.

Results and Discussion

To determine the thermal stability of ZnO@ZIF-8 composites, thermogravimetric analysis (TG) in air atmosphere was carried out. The weight loss below 400 ºC (~1.1%), as shown in Fig. 1, is the evaporation of adsorbed compounds in the surface of ZnO@ZIF-8 [17]. The significant weight loss (~21.4%) arose in the range of 400-600 ºC, because the decomposition of ZIF-8 were transformed to ZnO. When the temperature is above 600 ºC, ZnO loses weight slowly due to due to the crystallization of high temperature [16]. Therefore, the ZnO@ZIF-8 composites are stable below 400 ºC, and the sample begins to decompose above 400 ºC.

The purity and the phase of as-synthesized products were characterized by the X-ray diffraction (XRD) patterns. Fig. 2 is XRD curves of as-obtained products at different reaction environment, and suggests that a new phase forms with different experiment condition. In XRD curve of ZnO sample, the diffraction peaks at 31.77º, 34.41º and 36.25º are well matched with (100), (002) and (101) crystalline planes of ZnO (JCPDS Card No.36-1451) respectively. The result reveals that ZnO was prepared. In the XRD curve of ZnO@ZIF-8 sample prepared by ZnO powder reacting with 2-methylimidazole, we observed that the intensity of ZnO diffraction peak decrease, and the other diffraction peaks in the XRD curve can be indexed to the simulated ZIF-8. When the ZnO@ZIF-8 powder was calcined at 400 ºC for 120 min in N_2 atmosphere, and the sample of ZnO@ZIF-8-N_2 was obtained. It can be observed that the XRD curve of ZnO@ZIF-8-N_2 correspond to XRD pattern of ZnO@ZIF-8, suggesting that the lattice structure of the sample has not been destroyed at 400 ºC in N_2 atmosphere. Thus, it can be concluded that the sample of ZnO, ZnO@ZIF-8 composites and ZnO@ZIF-8-N_2 composites were successfully prepared by simple solution reaction and calcination.

Fig. 3 shows the SEM images of these products. it can be seen that ZnO powder is composed of the nano/

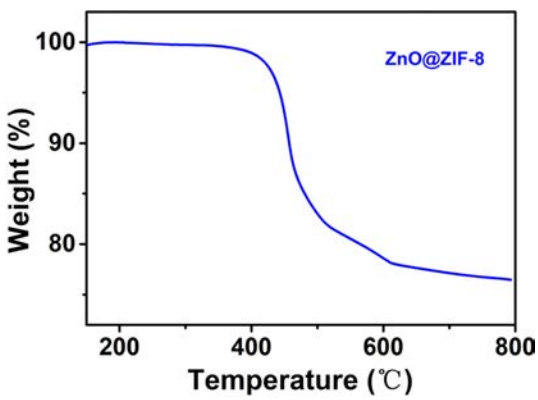

Fig. 1. TG curve of the samples.

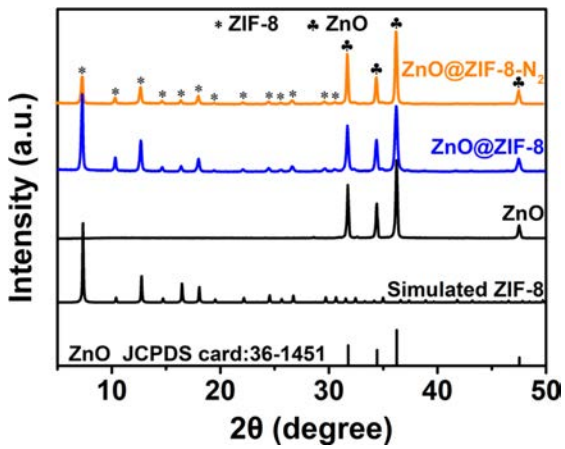

Fig. 2. XRD patterns of the samples.

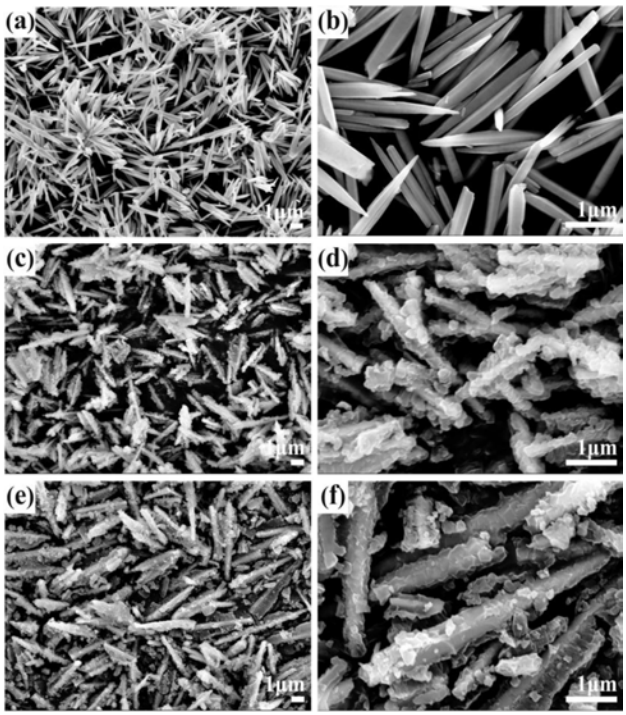

Fig. 3. SEM images of as-obtained products. the product ZnO nano/microrods (a, b); the sample ZnO@ZIF-8 nanostructured composites (c, d); the sample ZnO@ZIF-8-N_2 nanostructured composites (e, f).

microrods, with the length of ~2-5 μm and the diameter of ~80-300 nm, from the SEM image (Fig. 3(a) and Fig. 3(b)). After ZnO nano/microrods reacting with 2-methylimidazole, the part surface of ZnO were transformed into ZIF-8, and the ZnO nano/microrod surface was rough and decorated with different nanoparticles of 60-200 nm. The ZnO@ZIF-8 nano/microrods with rough surfaces were obtained (Fig. 3(c) and 3(d)). When the calcination temperature of ZnO@ZIF-8 is 400 ºC at N_2 atmosphere, the size and morphology of the ZnO@ZIF-8-N_2 have no obvious change (Fig. 3(e) and 3(f)). Therefore, ZnO@ZIF-8 nanostructured composites and ZnO@ZIF-8-N_2 nanostructured composites can be fabricated by ZnO nano/microrods reacting with 2-methylimidazole.

The UV-Vis spectra of ZnO, ZnO@ZIF-8 and ZnO@ZIF-8-N_2 samples are displayed in Fig. 4(a). ZnO shows absorption bands in the UV region and the onset of ZnO absorption edge is 390 nm, and it is similar to that reported in the literature [18, 19]. In comparison with ZnO powder, the stronger absorption of ZnO@ZIF-

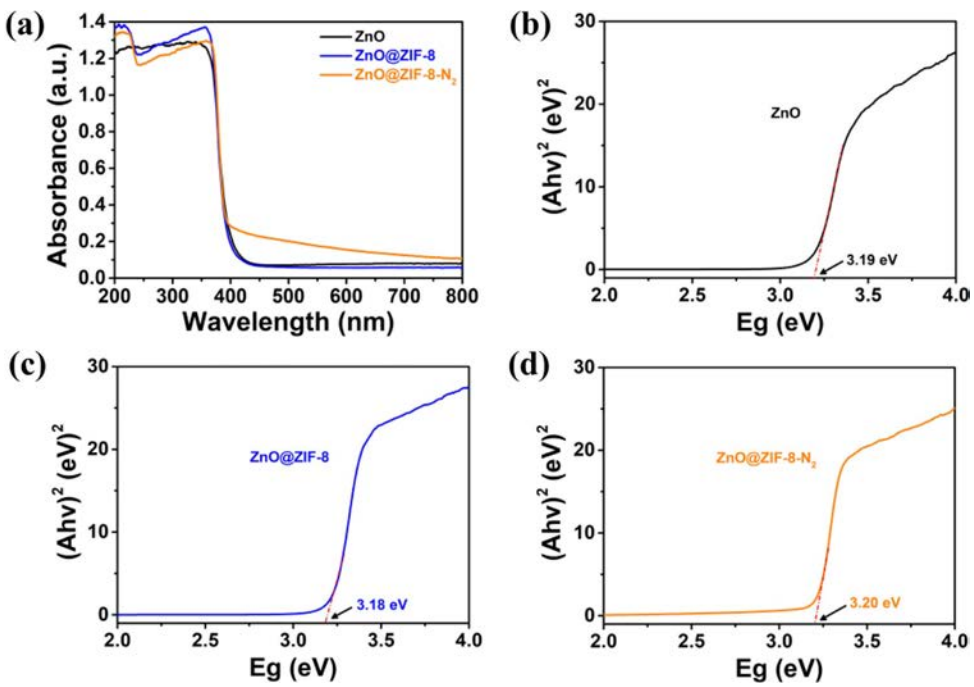

Fig. 4. (a) UV-vis absorption spectra of the samples; (b), (c) and (d) the plots of $(ahv)^{1/2}$ versus hv (d) of the samples.

8-N_2 and ZnO@ZIF-8 nanostructured composites was observed in the visible light range (390-780 nm). Using the equation [20, 21] $ahv = A(hv - Eg)^{1/2}$, the estimated band-gap energies (Eg) of ZnO powder, ZnO@ZIF-8 and ZnO@ZIF-8-N_2 are about 3.19 eV, 3.18 eV and 3.20 eV, as shown in Fig. 4(b), 4(c) and 4(d), respectively. It suggested that ZnO@ZIF-8-N_2 and ZnO@ZIF-8 nanostructured composites might display improved photocatalytic properties under visible light.

Fourier transform infrared (FTIR) spectra of ZnO, ZnO@ZIF-8-N_2 and ZnO@ZIF-8 over the wave number of 400-4000 cm^{-1} are presented in Fig. 5. The FTIR band at 489 cm^{-1} corresponds to the absorption peak of Zn-O bond [22]. When the part surface of ZnO were transformed into ZIF-8, the bands at 758, 1144 and 1,305 cm^{-1} are ascribed to imidazole ring [22], and the intensity of the bands at 1,444, 1,584, 2,927 and 3,133 cm^{-1} appears significant increase. When the calcination temperature of ZnO@ZIF-8 is 400 °C at N_2 atmosphere, the intensity of the bands at 759, 1,145, 1,306, 1,444, 1,584, 2,927 and 3,133 cm^{-1} appears significant decrease. The variations for the IR peaks further confirmed that the surface adsorption of ZnO@ZIF-8 is stronger than that of ZnO and ZnO@ZIF-8-N_2.

The photocatalytic performances of ZnO powder, ZnO@ZIF-8-N_2 and ZnO@ZIF-8 nanostructured composites are evaluated by the decomposition of MB dye, and MB dye is a general simulated pollutant in heterogeneous catalytic reactions. In order to establish the adsorption/desorption equilibrium, the MB solution was placed in the dark for 35 min before light irradiation. The photocatalytic activities have been recorded in Fig. 6. Fig. 6(a) shows the variation in MB absorption spectra with time under different visible light irradiation time and 20 mg of ZnO@ZIF-8 nanostructured composites as catalyst. It can be seen that the UV-Vis absorbance value of methylene blue solution decreases rapidly with extension of illumination time, and almost disappears after about 60 min. The degradation rate under visible light is 97.6%, suggesting that the solution of MB is effectively degraded by the ZnO@ZIF-8 nanostructured composites. For comparison, the catalytic degradation of methylene blue was also carried out under the same experimental conditions using ZnO powder, ZnO@ZIF-8-N_2 nanostructured composites as catalyst, and the photolysis experiment of MB solution without catalysts. Fig. 6(b) shows the change of C/C_0 (relative concentration of MB) with the illumination time of visible light over ZnO powder, ZnO@ZIF-8 nanostructured composites, ZnO@ZIF-8-N_2 nanostructured composites and blank solution of MB. After irradiation of visible light for 60 min, the absorption value of blank MB solution is not an obvious decrease. The ZnO@ZIF-8 nanostructured composites display much higher catalytic activity than other as-obtained samples, and MB degradation percentage reach to 97.6% after 120 min. When the ZnO powder and ZnO@ZIF-8-N_2 nanostructured composites were used as the catalysts, the MB degradation rate reached to 86.3% and 95.4%, respectively. It suggested that the activity of ZnO@ZIF-8 nanostructured composites shows a significant enhancement in photodegradation activity. Comparing these products [15], ZnO@ZIF-8 nanostructured composites have higher degradation performance, which indicates ZIF-8 on the surface of ZnO was an important factor in the improved photocatalytic activity. The improvement of the photocatalytic activity could be explained in terms of the following

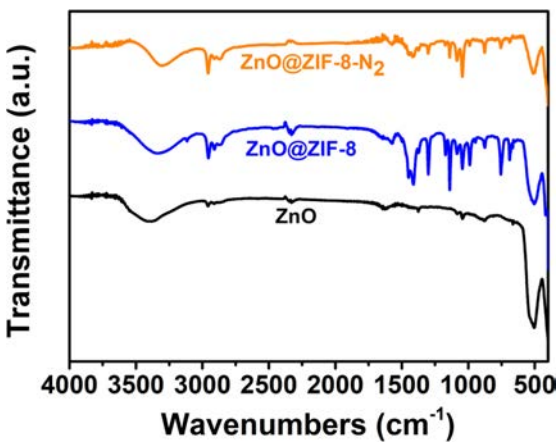

Fig. 5. FTIR spectra of the samples.

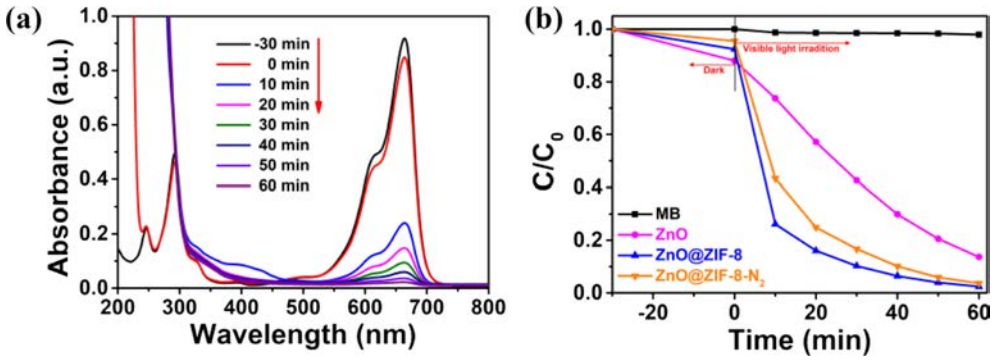

Fig. 6. Photocatalytic degradation of MB solution. (a) The change of UV-vis spectra of MB solution with time in the presence of ZnO@ZIF-8 nanostructured composites. (b) Photocatalytic properties of different samples under irradiation of visible light.

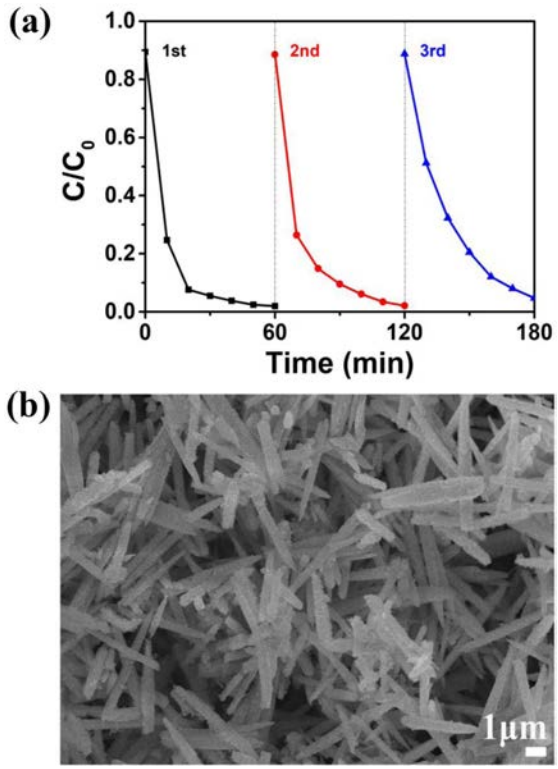

Fig. 7. (a) Three cycles in the photocatalytic decomposition of MB over ZnO@ZIF-8, (b) SEM image of the used ZnO@ZIF-8.

reasons. Firstly, the better photodegradation efficiency of the ZnO@ZIF-8 products may be due to rough surface of ZnO@ZIF-8 and the enhanced absorbance spectra of ZnO@ZIF-8, because of ZIF-8 coated on the surface of ZnO. Secondly, ZIF-8 on the ZnO@ZIF-8 surface prepared by the ZnO surface reacts to form ZIF-8 has the increase of surface area. Thirdly, Heterostructures of ZnO@ZIF-8 composites suppresses the recombination of photogenerated electron-hole pairs and accelerate the oxidation of organic molecules. Therefore, ZnO@ZIF-8 nanostructured composites exhibit higher catalytic activity than other samples.

A three cycle experiment of catalytic degradation of methylene blue solution was carried out to evaluate ZnO@ZIF-8 stability, which is an important index for the practical applications of the catalyst. Fig. 7(a) shows the three cycles of the change in the relative concentration C/C_0 of MB with irradiation time over ZnO@ZIF-8 catalysts. The value of degradation rate is 97.2, 96.3 and 93.7%, for the first, second and third runs, respectively. After three consecutive runs, there is only a slight loss of the photocatalytic performance, and it shows that ZnO@ZIF-8 catalyst has the high photocatalytic stability. Moreover, SEM inspection of the used ZnO@ZIF-8 (Fig. 7(b)) and fresh ZnO@ZIF-8 (Fig. 3(c) and Fig. 3 (d)) revealed it to have similar features, suggesting that it remained efficient and stable during MB degradation.

Conclusions

In summary, ZnO@ZIF-8 and ZnO@ZIF-8-N_2 nanostructured composites have been synthesized successfully by a simple solution reaction and calcination using the ZnO nano/microrods as precursor. Among them, ZnO@ZIF-8 nanostructured composites exhibited enhanced photocatalytic performance in the MB degradation under irradiation of visible-light, and the degradation rates of MB solution reached to 97.6%. Finally, the possible photocatalytic mechanisms of ZnO@ZIF-8 nanostructured composites were discussed. It is believed that ZnO@ZIF-8 nanostructured composites may be a potential photocatalyst for the treatment of industrial wastewater containing organic pollutants.

Acknowledgements

This research was supported by first-rate discipline construction of applied chemistry of Shanghai University of Engineering Science (No. 2018xk-B-06), SUES Sino-foreign cooperative innovation center for city soil ecological technology integration (2017PT03), Capacity building project of Some Local Colleges and Universities in Shanghai (No.17030501200) and the Foundation of Shanghai University of Engineering Science (Grant no. 2012gp13, E1- 0501-15-0105).

References

1. B.H. Sun, Q.Q. Li, M.H. Zheng, G.J. Su, S.J. Lin, M.G. Wu, C.Q. Li, Q.L. Wang, Y.M. Tao, L.W. Dai, Y. Qin and B.W. Meng, Environ. Pollut. 265 (2020) 114908.
2. K. Vellingiri, K. Vikrant, V. Kumar and K.-H. Kim, Chem. Eng. J. 399 (2020) 125759.
3. Y. Xu, C. Zhang, P. Lu, X. Zhang, L. Zhang and J. Shi, Nano Energy. 38 (2017) 494-503.
4. M. Zhang, Q. Shang, Y. Wan, Q. Cheng, G. Liao and Z. Pan, Appl. Catal. B. 241 (2019) 149-158.
5. R.Y. Wu, H.B. Song, N. Luo and G.J. Ji, J. Colloid. Interface Sci. 524 (2018) 350-359.
6. A. Kumar, A. Kumar and V. Krishnan, ACS Catal. 10 (2020) 10253-10315.
7. T.K. Maji, D. Bagchi, P. Kar, D. Karmakar and S.K. Pal, J. Photochem. Photobiol. A. 332 (2017) 391-398.
8. B.G. Shohany and A.K. Zak, Ceram. Int. 46[5] (2020) 5507-5520.
9. O. Mangla and S. Roy, Solid. State. Phenom. 287 (2019) 75-79.
10. W.L. Zhang, Y.G. Sun, Z.Y. Xiao, W.Y. Li, B. Li, X.J. Huang, X.J. Liu and J.Q. Hu, J. Mater. Chem. A. 3[14] (2015) 7304-7313.
11. B. Bajorowicz, M.P. Kobylanski, A. Golabiewska, J. Nadolna, A. Zaleska-Medynska and A. Malankowska, Adv. Colloid. Interface. Sci. 256 (2018) 352-372.
12. W.F. Li, Y.G. Sun and J.L. Xu, Nano-Micro Lett. 4[2] (2012) 98-102.
13. H. Kim, W. Kim, J. Park, N. Lim, R. Lee, S.J. Cho, Y. Kumaresan, M.-K. Oh and G.Y. Jung, Nanoscale. 10[45] (2018) 21168–21177.

14. L. Tian, Y.X. Sun, H.L. Huang, X.Y. Guo, Z.H. Qiao, J.Q. Meng and C.L. Zhong, Chemistry Select. 5[8] (2020) 2401-2407.
15. X.B. Yang, Z.D. Wen, Z.L. Wu and X.T. Luo, Inorg. Chem. Front. 5[3] (2018) 687-693.
16. X.B. Wang, J. Liu, S. Leong, X.C. Lin, J. Wei, B. Kong, Y.F. Xu, Z.-X. Low, J.F. Yao, and H.T. Wang, ACS Appl. Mater. Interfaces. 8 (2016) 9080-9087.
17. W.B. Shen, P.S. Tang, S. Cheng and C.Y. Lv, Integr. Ferroelectr. 206[1] (2020) 10-16.
18. Y.G. Sun, J.Q. Hu, N. Wang, R.J. Zou, J.H. Wu, Y.L. Song, H.H. Chen, H.H. Chen, Z.G. Chen, New. J. Chem. 34[4] (2010) 732-737.
19. C. Liu, F.L. Meng, L. Zhang, D.T. Zhang, S.T. Wei, K. Qi, J.C. Fan, H.Y. Zhang, X.Q. Cui, Appl. Surf. Sci. 469 (2019) 276-282.
20. J.W. Bai, X.M. Li, Z.W. Hao and L. Liu, J. Colloid. Interface. Sci. 560 (2020) 510-518.
21. M.Z. Sun, P.Y. Guo, M. Wang and F.Y. Ren, Opt. Int. J. Light Electron Opt. 199 (2019) 163319.
22. G.J. Ren, Z.M. Li, W.T. Yang, M. Faheem, J.B. Xing, X.Q. Zou, Q.H. Pan, G.S. Zhu, Y. Du, Sensor. Actuat. B-Chem. 284 (2019) 421-427.